Journal of Civil Engineering and Applications

E-ISSN: 2707-8396
P-ISSN: 2707-8388
JCEA 2023; 4(1): 11-20
Received: 08-11-2022
Accepted: 15-12-2022

HHM Darweesh
Refractories, Department of Ceramics and Building Materials, National Research Centre, Cairo, Egypt

Corresponding Author:
HHM Darweesh
Refractories, Department of Ceramics and Building Materials, National Research Centre, Cairo, Egypt

Utilization of sugarcane bagasse ash at the expense of feldspar in the production of ceramic porcelain insulators

HHM Darweesh

Abstract
Sugarcane bagasse ash (SCBA) which is an industrial waste was partially substituted at the expense of feldspar (F) to produce ceramic porcelain insulators. Raw materials were characterized for their chemical composition and thermal behavior. Porcelain insulator batches containing various proportions of SCBA (0-35 wt.) were fired at different firing temperatures of 1050, 1100, 1150, 1200, 1250 and 1300 °C for two hours soaking. The fired units were conducted for water absorption, apparent porosity, bulk density, bending strength, crushing strength, dry and firing shrinkages. Results showed that SCBA had a lower 68.19% SiO_2 content (68.19%) than feldspar (74.22%), but feldspar had a lower alkali content (7.24%) than SCBA (7.82 wt%). Water absorption was decreased with increasing both SCBA content and firing temperatures. Water absorption values are too small, and this was confirmed by the results of apparent porosity. This in turn was reflected positively on the bulk density and mechaanical properties. Dry shrinkage was unchanged, wlile firing shrinkage was slightly increased with both SCBA and firing temperatures. Furthermore, the partial replacement of F by SCBA up to 35 w% achieved the better results comparing with those of the control batch. The optimum firing temperature and SCBA content are 300 ºC and 35%, respectively.

Keywords: Insulators, feldspar, sugarcane bagasse ash, firing temperature, water absorption, density, strength, shrinkage

1. Introduction
Porcelain insulators have been widely used due to its safe electricity transmission though the emergence of new insulators as plastics and composites [1]. Electrical insulators are one of the electric power transmission systems, in which the quality limits the efficiency of electricity transmission and distribution [2, 3]. The cost of these insulators is too low, and it can resist both high temperatures, and severe environment, and moreover they have too long lifetime but not sensitive to firing temperatures [2, 4-6]. Electrical porcelain insulators are ceramic materials manufactured by heating pressed homogenized powders of raw materials primarily clay, feldspar, and quartz in a kiln up to 1200 and 1400 °C [7, 8]. Clay is a source of alumina, which, together with quartz and fluxing element, can form mullite and glassy phase during the firing, and also it provides the plasticity. Mullite ($3Al_2O_3$, $2SiO_2$) is the main product phase formed on firing kaolinite clay at high firing temperatures 750-850 ºC). Moreover, it has a low thermal expansion coefficient and dielectrical loss [9]. Formation of these phases improves and enhances the mechanical and dielectric strength of the porcelain insulators [10, 11].
Feldspar acts as the flux agent where it is a source of alkaline oxides such as Na_2O and K_2O to produce a low-viscosity melt during firing at high firing temperatures contributing to a decrease in the firing temperature [12]. Depending on the chemical composition, feldspars start melting above 1000 °C to form a liquid phase and fill the pores of the ceramic composition by a capillary effect. This is promoting the vitrification and densification of the porcelain product at the end of the firing process [1, 13]. Feldspar often showed lower fluxing oxides which always requires a high sintering temperature to form a vitreous phase that can block the open pores present in the ceramic body. This contributes to the formation of the required amount of mullite phase [14, 15]. Quartz maintains a porcelain structure and regulates the ratio of SiO_2 to Al_2O_3 for the formation of mullite. So, it is resistant to melt at lower firing temperatures (<1300 °C) [7]. The grain size particle of quartz plays a vital role in the sintering temperature and strength development of porcelain producuts [16, 17].

Quartz with grain size < 45 μm always improves and enhances mechanical and dielectric strength properties by increasing its dissolution, minimize thermal expansion stresses, and smooth out the volume changes of α to β quartz transition [7, 12, 16, 18-20]. Consequently, the microstructure, electrical and mechanical properties of porcelain insulators are mainly depending on its chemical and mineralogical composition paralel with the conditions of preparation, mixing, and sintering [12, 14, 17, 21, 22].

In ceramic industry, both energy and cost of raw materials are very essential for the sustainable development of porcelain electrical insulators must be reduced. This may be achieved by using fast firing cycles with available locak raw materials and fluxing agents as feldspar [23, 24]. The high-grade feldspar minerals have recently a high cost compared with those of clay and quartz [25]. The ceramic industries in Ethiopia produce porcelain insulators from imported clay materials, and the locally mined feldspars that display Feldspars having a very low fluxing ability are not suitable for the production of ceramic insulators [23]. So, it is necessary to explore alternative locally available ceramic raw and/or waste materials of high fluxing ability which could be used as a substituent for feldspar in the porcelain bodies. Previous studies have identified numerous silicate-based wastes such as soda-lime glasses [26], blast furnace slag [25, 27, 28], metallurgical slags [29], rice straw ash and/or rice husk ash [30], silica fume [31], and fly ash [32], cement kiln dust waste [33, 34] as potential partial replacement of feldspar and showing promise for improving the insulator physical and/or microstructural properties and lowering the firing temperatures, leading to cost minimization.

Recently, sugarcane bagasse ash (SCBA) has been utilized in building and construction materials at a certain level to improve both physical and mechanical properties. This reduces the CO_2 emission in the atmosphere [35–37]. In Egypt, the accumulation of large quantities of SCB in the environment polluted it due to the rapid growth of sugar industries. SCBA produced during the use of SCB as fuel in boilers for energy co-generation, where one ton of SCB may generate 25 kg of SCBA [38, 39]. It is mainly composed of SiO_2 and traces of Al_2O_3, Fe_2O_3, CaO, and K_2O which acting as fluxing agents. The overall chemical composition is much similar to the common natural aluminosilicate raw materials that are used in the manufacture of ceramics [40-42]. Currently, the SCBA is usually dumped on open air leading to detrimental environmental effects. The potential of SCBA as a substitute for quartz in the preparation of red ceramics were discussed [7, 38, 41-44]. Furthermore, the higher amount of K_2O in SCBA has been proved that it could be used as a potential supplement to natural feldspar to enhance its alkali oxides content for porcelain insulator production at lower firing temperatures. Hence, incorporation of SCBA in the ceramic product can have several advantages including saving natural raw materials, lowering the energy consumption during subsequent processing, and mitigating environmental pollution [40-46].

Therefore, this study investigates the effect of partial substitution of feldspar by SCBA to produce high quality porcelain insulators. The physical properties in terms of water absorption, apparent porosity and bulk density as well as mechanical properties in tems of bending and crushing strengths were investigated. Also, the dey and firing shrinkage was evaluated.

2. Materials and Methods

2.1 Raw Materials

An experimental design was formulated to investigate the influence of SCBA content on both physical and mechanical properties of the prepared porcelain insulator products that were fired at various firing temperatures. The raw materials used in the current study are clay, sand and feldspar. The clay sample was taken from Toshka region (TC). Toshka region is located on latitude 20º 30˙ N and longitude 31º 53˙ E at 250 km south of Aswan which was contributed to the Upper Cretaceous age (Fig. 1).

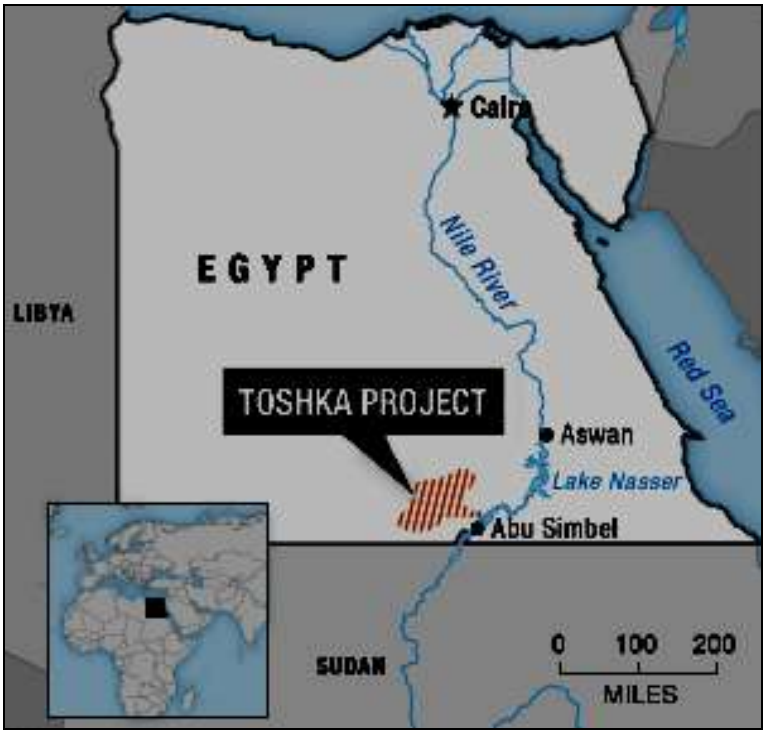

Fig 1: Toshka region from which the clay sample was taken.

The selected clay deposit is belonging to El-Dakhla Shale Formation. About 15 kg clay was collected from the 85th km north of Aswan/Abu-Semple asphaltic road. It is dark yellowish grey. The TC sample was first well dried in an open air for two days and in a suitable furnace at 110 ºC for another two days. It then crushed, ground and quartered to have a representative sample which was fine ground to pass a 200 mesh sieve. Feldspar (F), quartz sand (QS) from El-Hekma firm and a broken fired ceramic waste with the commercial name Grog (G) were obtained from the Arab Ceramic Company which is commercially known as Aracemco, Egypt. The used feldspar is essentially a mixture of two feldspars namely, orthoclase-potash feldspar, $KAlSi_3O_8$ or $K_2O.\ Al_2O_3.\ 6SiO_2$ and albite-soda feldspar, $NaAlSi_3O_8$ or $Na_2O.\ Al_2O_3.\ 6SiO_2$, with small amounts of mica and quartz. The feldspar is often extracted by normal quarrying or mining with visual control over the extracted material at the quarry face [47]. The sugarcane bagasse (SCB) sample was provided by a local sugarcane juice shop, Egypt. The SCB was first processed and washed with running water, and also with distilled water. Then, it let to dry under sun and open air for three days. The dried SCB was subjected for firing at 850 ºC for two hours soaking to produce what is known as sugarcane baggasse ash (SCBA). Then, the resulting SCBA was screened to pass through 300 µm standard sieve. The chemical analysis using the X-ray fluorescence technique (XRF) and the particle size distribution of the starting raw materials are shown in Tables 1 and 2, respectively. The loss of ignition (LOI) was determined from the mass difference of samples heated at 105 °C and 1000 °C for 2 hours. The suggested ceramic batch composition from the above mentioned raw materials is given in Table 3. The base batch composition was well mixed in an agate ball mill for one hour using the wet method, let to dry and thoroughly crushed and ground well again to pass through 200 mesh sieve to be the stock base ceramic porcelain batch.

Table 1: Chemical analysis of raw materials, wt.%

Materials Oxides	TC	QS	F	SCBA
SiO_2	52.51	97.43	74.72	68.19
Al_2O_3	30.47	0.71	14.73	13.18
Fe_2O_3	2.32	0.07	1.75	4.19
CaO	0.75	0.41	0.73	1.26
MgO	1.36	0.07	----	1.36
MnO	0.08	0.02	0.04	0.14
Na_2O	1.17	0.11	3.21	3.03
K_2O	1.13	0.16	4.03	4.79
F_2O_5	0.42	0.03	----	0.81
TiO_2	1.07	0.13	0.06	0.27
LOI	8.72	0.86	0.73	2.78
Total	100	100	100	100

Table 2: Particle size analysis of the used raw materials, µm.

Materials	Particle size distribution, µm					
Size	> 63	63-16	16-8	8-2	< 2	Total
TC	1.19	1.24	2.41	5.15	90.01	100
SS	0.11	0.12	0.63	2.81	96.33	100
F	0.15	1.03	1.07	1.24	96.51	100
SCBA	0.11	1.01	0.41	1.15	97.32	100

Table 3: Batch composition of the different ceramic insulators, wt.%.

Materials Oxides	TC	SS	F	SCBA
B0	50	15	35	0
B1	50	15	30	5
B2	50	15	25	10
B3	50	15	20	15
B4	50	15	15	20
B5	50	15	10	25
B6	50	15	5	30
B7	50	15	0	35

Figure 2 demonstrates the DTA-TGA thermograms of TC sample. The endothermic peak at the temperature range of 700-900 ºC is due to the calcination of limestome. The two endothermic peaks at the temperature range 100-120 and 500-600oC are due to the evaporation of the absorbed and structural or hygroscopic water, respectively. The endothermic peak at the temperature range 500-600oC is due to the conversion of kaolinite (AS_2H_2) to metakaolin (A_2S_2), which in turn is converted to mullite phase (A_2S_2) at 980 ºC [48] as follows:-

$$AS_2H_2 \rightarrow AS_2 \rightarrow A_2S_2 \quad (1)$$

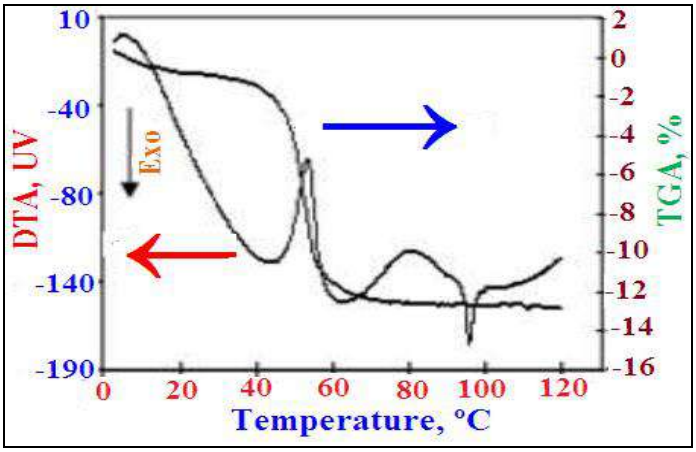

Fig 2: The DTA and TGA thermograms of TC sample.

Samples of TC, F, Q, and SCBA were ball milled using a suitable laboratory ball mill. The milled raw materials were then sieved till pass from 200 mesh sieve (63 μm) [49, 50].

2.2 Preparation

The base batch has the symbol B0. Then, the SCBA was partially substituted at the expense of feldspar. There are six powdered ceramic batches were prepared incorporated SCBA as 100:0, 98:2, 96:4, 94:6, 92:8 and 90:10 mass% at the expense of feldspar with symbols B0, B1, B2, B3, B4 and B5, respectively. The batches were mixed well in a gate ball mill for one hour using the wet method, dried at 105 ºC for three days, and then ground to pass a 200 mesh sieve to obtain the same homogeneity of all batches. Five disc-shaped samples of 1 cm diameter and 1 cm thickness were prepared for the physical properties in terms of water absorption (WA), bulk density (BD) and apparent porosity (AP). Also, five rod or rectangular shaped samples of 2.5 x 2.5 x 7 cm^3 were prepared for dry and firing shrinkage as well as for bending or fluxural strength. Afterthat, five cube samples of 2.5 x 2.5 x 2.5 cm^3 for crushing strength were moulded. Molding of specimens were carried out using a suitable hydraulic presser under a shaping pressure of 20 KN/mm^2 with the help of water as a binder. After demoulding, the samples were let to dry in air at 23 ± 2 ºC for 48 hours, and then let to dry at 105 ºC in a suitable oven till a constant weight to ensure the complete elimination of free and crystallized water and also to avoid the cracks during firing. The firing process was carried out using a slow rate furnace Mod. Vecstar with a heating rate 5 ºC/min. The firing temperatures were 1100, 1150, 1200, 1250 and 1300 ºC with one hour soaking [51]. The fired specimens were left to cool slowly inside the furnace over night to room temperature. The optimum firing temperature of each ceramic batch was estimated.

2.3 Methods

2.3.1 Physical or Densification Parameters

The ceramic or densification parameters [52, 53] in terms of water absorption (WA), bulk density (BD) and apparent porosity (AP) could be determined from the following equations:

$$W.A, \% = (W1-W2) / (W3) \times 100 \quad (1)$$

$$B.D, g/cm^3 = (W3) / (W1-W2) \quad (2)$$

$$A.P, \% = (W1-W3) / (W1-W2) \times 100 \quad (3)$$

2.3.2. Mechanical properties

The mechanical properties in terms of bending or flexural strength (FS) and crushing strength (CS) [11, 12] of the green and fired units [54-56]. The bending strength could be carried out using the three point adjustments system (Fig. 3) and is calculated from the following equations:

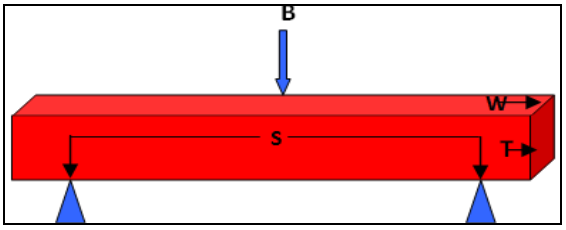

Fig 3: Schematic diagram of bending strength, B: Beam or loading of rupture, S: Span, W: Width and T: Thickness.

$$BS, kg/cm^2 = 3\ BS\ kg/cm^2/2W.T\ Kg/cm^2/\ 10.2\ MPa \quad (1)$$

Where, BS is the bending strength, kg/cm^2, B is the bending load of rupture, kg, S is the Span (the distance between the two lower beams, 5 cm), W is the width of the sample, cm and T is the thickness of the sample, cm. The crushing strength of samples at the various firing temperatures could be determined using the following relation:

$$CS = (D)(L)\times(w) = kgcm2/10.2\ MPa \quad (5)$$

Where, CS: crushing strength $kgcm^2$, D: load kg, L and W are the length and width of the samples, respectively.

The XRF analysis is equipped by a modern wavelength dispersive Spectrometer (WD-XRF, 2005, Netherlands). The particle size distribution of the starting raw materials was carried out using the sieve analyzing method. The DTA-TGA thermograms of T-Clay sample which was carried out using NETZSCH Geratebae GmbH Selb, Bestell No. 348472c at a heating rate 10 °C/min. up to 1000 °C. The XRF analysis was carried out in the National Research Centre while the particle size distribution was achieved in the Metals Institute, El-Tabine, Cairo, Egypt. The loss on ignition of the used raw materials (LOI) was measured due to the mass difference of samples fired up to 1000 °C for two hours [57]. Thermal analysis of TC was carried out by differential thermogravimetric analysis (TGA) coupled with Differential Thermal Analysis (DTA) [58].

3. Results and Discussions

3.1 Chemical compositions analysis of raw materials

The chemical composition and LOI of raw materials are shown in Table 1. TC is comprised mainly of SiO_2 (52.51%) and Al_2O_3 (30.47%) with a low percentage of other oxides as CaO (0.75%), MgO (1.36%), MnO (0.08), TiO_2 (1.07%) and P_2O_5 (0.42%) and also fluxing oxides as Na_2O (1.17%) and K_2O (1.13%). The ratio of SiO_2 to Al_2O_3 was 1.72. This value closes to a pure kaolinitic clay and slight deviations indicating the presence of unweathered quartz [11, 58]. Hense, the used clay was kaolinitic clay that was confirmed by the ratio of SiO_2 / Al_2O_3 and fulfilled the required purity for sufficient mullite phase during the sintering of the prepared porcelain products [41, 59]. The small amount of Fe_2O_3 (2.32%) in TC which is within the standard requirement for porcelain insulator production, is expected to enhance the action of the alkali fluxes to melt at lower temperatures [16, 21, 41, 60]. The amount of alkaline oxides (K_2O and Na_2O) is (2.30%), which was comparable with commonly used china clay, but higher than that of ball clay [60]. Even though their amount is low, it is expected to decrease the sintering temperatures. The LOI of TC (8.72%) is comparable to kaolinitic clays, and is mainly containing clay minerals, hydroxides, and organic matter [38, 61].

The feldspar is containing SiO_2 (74.72%) and Al_2O_3 (14.73%) as principal oxides. This implies that the feldspar was suitable for the production of porcelain bodies (66.3-79.5%) [62]. However, the percentage of fluxing oxides, K_2O and Na_2O (7.23%) are little lower than that required for the production of porcelain insulator (>12%) [60]. This demonstrated that feldspar must be used with a higher amount and at higher firing temperature to achieve the optimum glassy phase in a porcelain body [4].

The Fe_2O_3 in feldspar is 1.75% which is much higher than the maximum allowable limit (.03). This lower amount

would contribute to wanted variations of the color towards grey rather than white and cause bloating due to the escape of entrapped gases during sintering [20]. Sol, the chemical composition of F is in a good agreement with those reported in some studies [20, 23], and fulfill the chemical purity requirement of feldspars for porcelain insulator fabrication [23]. The chemical analysis also showed that QS confirmed the presence of a higher amount of SiO_2 (97.43%) as it is the major component of sand fractions [63]. The QS fulfilled the required specification for quartz (97.0-99.1%) to be suitable for the production of porcelain product [62]. However, the QS may be utilized for the fabrication of porcelain insulators by using an optimized amount and reduction of the grain size to the requisite level, since the grain size of quartz primarily determines its dissolution rate and subsequent use as a filler in porcelain compositions and to increase the strength in a porcelain body [64].

The major oxides in SCBA was SiO_2 (68.19%), Al_2O_3 (13.18%) and Fe_2O_3 (4.19%), while the other oxides K_2O (4.79%), Na_2O (3.03%), CaO (1.26%), and MgO (1.36%) were also present in relatively significant proportions and comparable to that in F. So, the overall chemical composition of SCBA was in a good agreement that it could potentially be used as an alternative to partially substitute F. Furthermore, it is expected that the higher content of the alkaline oxides (K_2O and Na_2O) in SCBA (7.82%) compared to that in F (7.23%) may contribute to decrease the sintering temperatures. This in turn decreased the energy cost of fabrication [22]. The higher LOI (2.78%) in SCBA compared to the in F (0.73%) indicated the presence of unburnt carbon [65]. Based on the analysis of chemical composition, partial replacement of F by SCBA appears feasible even if the level of Fe_2O_3 needs some pretreatment for its reduction. From the previous discusion it could be concluded and confirmed that SCBA was more or less similar in mineralogical composition to that of F.

3.2 Physical properties

It is well known that water absorption is considered to be an important evidence for the quality and durability of ceramic products, which accurately defines the class to which the final product belongs [18, 29]. Figures 4-6 show the data of water absorption, apparent porosity and bulk density of the various fired ceramic insulators as a function of insulator batches (B0-B70. Generally, as the firing temperature increasesd, the densification parameters of the fired units in terms of water absorption, apparent porosity and bulk density evidently improved, where both water appsorption and apparent porosity decreased, while bulk density increased. This in turn reflected positively on the mechanical properties [2, 9, 13, 27]. On the other side, as the SCBA content increased up to 35 wt. % at the expense of F, the water absorption and apparent porosity gradually also decreased more, whilst the bulk density increased. The same trend was displayed with all firing temperatures and SCBA content up to 35% SCBA. This is mainly due to the formation of new phases resulting from the thermal reactions during firing either through decomposition and/or recombination changes [19, 33], i.e. during firing, the main crystalline phases in the green bodies were completely replaced by the formation of new amorphous and crystalline phases. Additionally, the melting action of feldspar which controls the thermal reactions and phases conversion of the insulator components in the liquid phases [7, 14, 45]. Furthermore, the presence of high amounts of fluxing oxides in clay and SCBA increased the rate of thermal reactions and liquid phase formation, which in turn flows directly and settled inside the pore structure of the fired products. On solidification, a product of more compact and glassy appearrance was formed [9, 19, 27]. The water absorption as well as apparent porosity decreased as the SCBA content and firing temperature increased. This often continued up till 35 wt. % SCBA [14, 33, 45]. This means that the addition of high amounts of SCBA into the insulator ceramic bodies is desirable due to its positive action on the physical properties of the formed insulator ceramic products. The insulator product containing 35% SCBA achieved the lowest values of water absorption and apparent porosity, and also the highest value of bulk density, respectively nearly at all firing temperatures compared with the other values of the other different insulator batches. Consequently, the insulator batch incorporating SCBA completely without F could be selected to be the optimum batch for insulator, i.e. the F could be replaced completely by SCBA without any adverse effect.

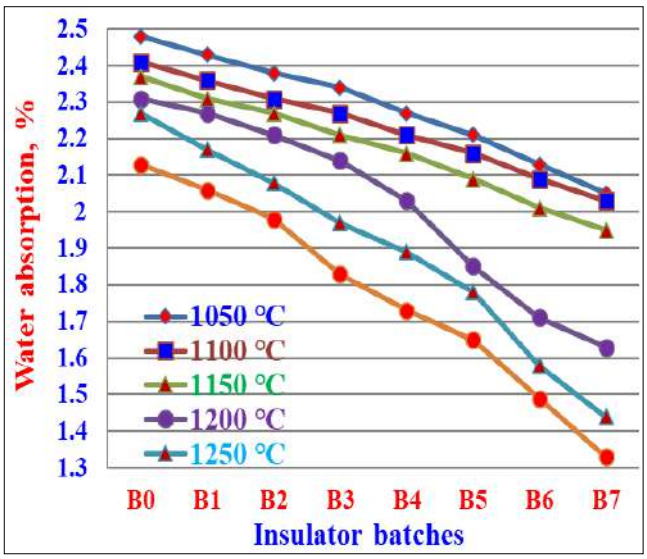

Fig 4: Water absorption of the various fired ceramin insulator batches at different firing temperatures.

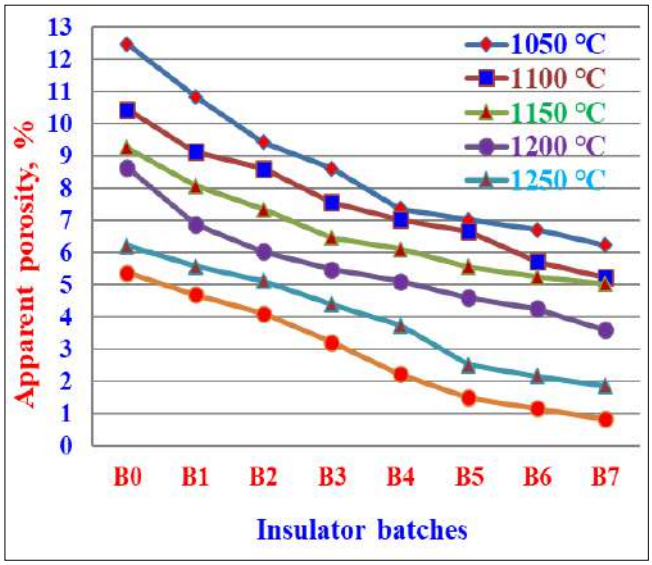

Fig 5: Apparent porosity of the various fired ceramin insulator batches at different firing temperatures.

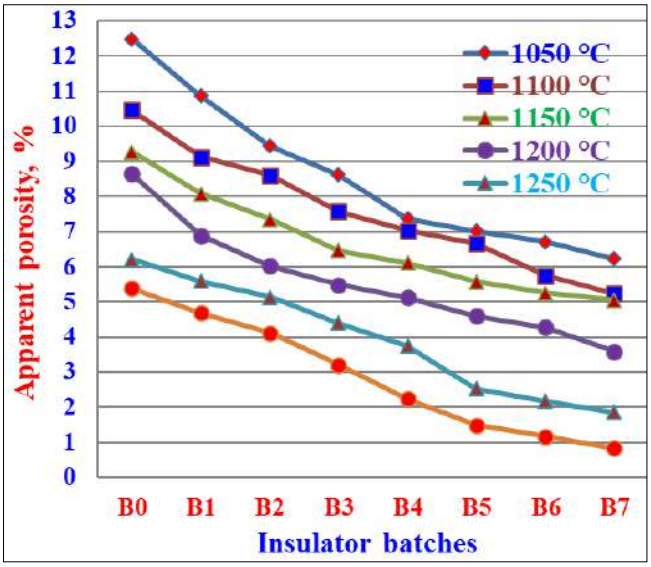

Fig 6: Bulk density of the various fired ceramin insulator batches at different firing temperatures.

3.3 Mechanical properties

3.3.1 Green bending strength

The bending strength of the green (dried or unfired) samples was plotted as a function of SCBA content in Fig. 7. The results revealed that the green bending strength of the control (B0) was slightly improved and increased with the gradual substitution of the very fine SCBA waste at the expense of feldspar. The green bending strength of the base batch (B0) recorded 1.52 MPa, while that of the batch containing 35% SCBA waste (B7) was 2.86 MPa. This represents a higher improving rate. This is mainly attributed to that the SCBA waste contains high percentage of fluxing oxides than F that iimproved both workability and green bending strength of the bodies containing it [48, 70].

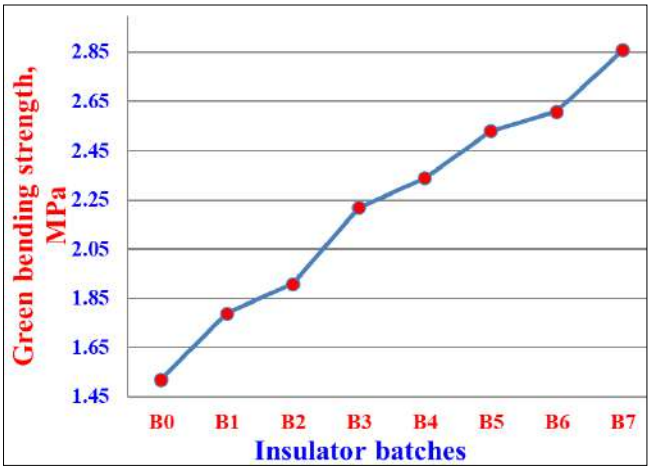

Fig 7: Green bending strength of the various unfired ceramin insulator batches.

3.3.2 Fired bending strength

The bending strength of the fired ceramic insulator units was plotted as a function of firing temperature in Fig. 8. Results illustrated that the bending strength of the fired bodies increased as both the SCBA waste content increased up to 35 wt. % and also as firing temperature increased up to 1300 °C. The fired ceramic bodies containing 35 wt. % SCBA waste (B7) at the maturing temperature of 1300 °C achieved bending strength value of 36.13 MPa compared with that of the base batch (B0) fired up to 1300 °C which recorded only 33.86 MPa, i.e. the improvements in bending strength value are equal to 6.7%. The mechanical properties of the fired ceramic units are dependent on the porosity, crystallininity and grain size of the newly formed phases. Hence, the grain size of the starting raw materials must be very fine to give considerable low particle boundaries which in turn resulted on low porosity [7, 9, 20, 33, 71]. This would be enhanced with the formation of glass phases [8, 45].

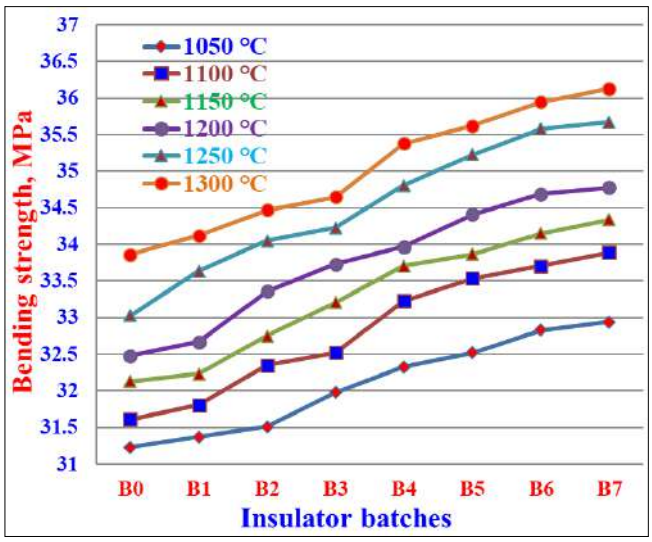

Fig 8: Bending strength of the various fired ceramin insulator batches at different firing temperatures.

Moreover, the rate of either densification or strength of the fired ceramic units could be increased by the addition of SCBA waste to reduce the total porosity of the formed glassy matrix during firing which solidifies on cooling. This in turn could cement all the unmelted and/or unreacted particles and crystals together to give good mechanical properties for the resulted units [7, 8, 33]. The influence of alkalies and earth alkalies in SCBA waste can alter the relative amounts of the formed liquid phases and lower the viscosity of the liquid. The used intimate mixing improves the latter process and reduces the maturing temperatures [8, 9, 20, 45].

3.3.3 Crusing strength

Crushing strength of the ceramic insulators batches containing various ratios of SCBA at the expense of F fired at different firing temperatures is plotted as a function of SCBA content in Fig. 9. Generally, crushing strength of the prepared fired ceramic insulators continuously increased with SCBA content up to 35 wt.%. This is due to that the presence of SCBA in the ceramic ingredients body improves and enhances the formation of glassy phase, but reduces its viscosity during sintering. On cooling, the glassy matrix solidifies and cements all the unmelted particles together. As a result, a ceramic insulator product of high mechanical properties could be obtained compared with those containing no SCBA [7, 9, 14, 33, 45]. Also, the crushing strength increased with the increase of firing temperature up to 1300 °C. This is mainly attributed to the increase of glassy or liquid phase that improves the thermal reactions between the various ingredients. This will lead to the formation of well-developed crystals [7, 33, 48, 71]. On the other side, as the SCBA content increased, the crushing strength of all

ceramic products gradually increased even with the increase of firing temperature up to 1300 °C. This may be contributed to that the higher amount of SCBA encourages the suitable contact between the various ceramic particles to react normally with each other and with those of SCBA. This in turn led to a promotion in the rate of the formed glassy phase. So, the new phases that responsible for the enhancing of mechanical strength were increased. In addition, the migration of gases through the matrix created a ceramic body with too low porosity, which reflected positively on the mechanical properties [7, 43, 45, 48, 71]. Hence, the results of densification properties of all samples are in a good agreement with those of mechanical strength. Accordingly, the optimum ceramic products are those containing 35 wt.% SCBA fired at 1300 °C.

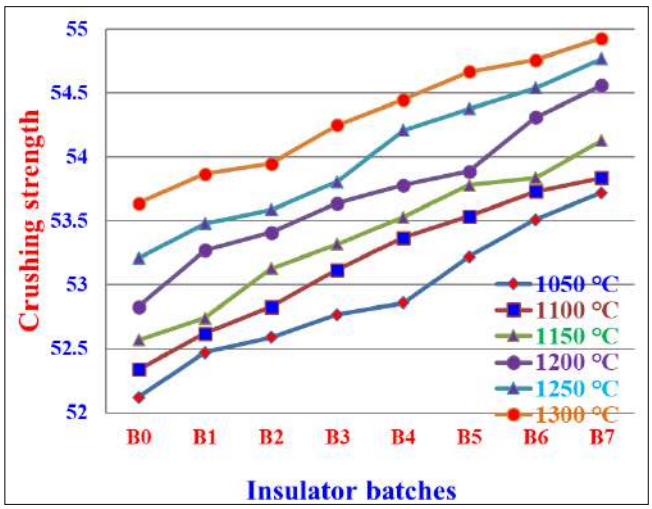

Fig 9: Crushing strength of the various fired ceramin insulator batches at different firing temperatures.

3.4 Dry and firing shrinkage

The dry and firing shrinkage of the various ceramic insulators units are drawn versus firing temperatures in Fig. 10. The dry shrinkage of all ceramic insulator bodies seemed to be unchanged, i.e. all are equal to zero. As the firing temperature increased, the firing shrinkage slightly enhanced [66-69]. The ceramic insulator units containing no SCBA, i.e. containing F only (B0) exhibited the lowest firing shrinkage values. With those incorborating SCBA (B1-B7), the firing shrinkage gradually and slightly increased. This trend was achieved with all firing temperatures. The lower values of firing shrinkage are mainly due to the removal of residual and combined water contents, but the higher values are due to the migration of gases from the dissociation of carbonates (CO_2) and sulfates (SO_3) [45, 68, 69]. Furthermore, the presence of larger amounts of CaO and alkali oxides in SCBA tends to lower the melting point of the fired articles that contributed to the formation of large amounts of glassy phase. This is the main reason of the continuous increase of the firing shrinkage of ceramic insulator bodies containing SCBA [7, 9, 14, 34, 43, 45]. However, the firing shrinkage of ceramic insulator units containing SCBA lies in the permissible limits in all-standard specifications. Hense, the dry and firing shrinkage of the prepared insulator ceramic units are in a good agreement with those of densification and mechanical properties. Therefore, the additin of SCBA at the expense of F in the ceramic insulator articles achieved the same results as F alone.

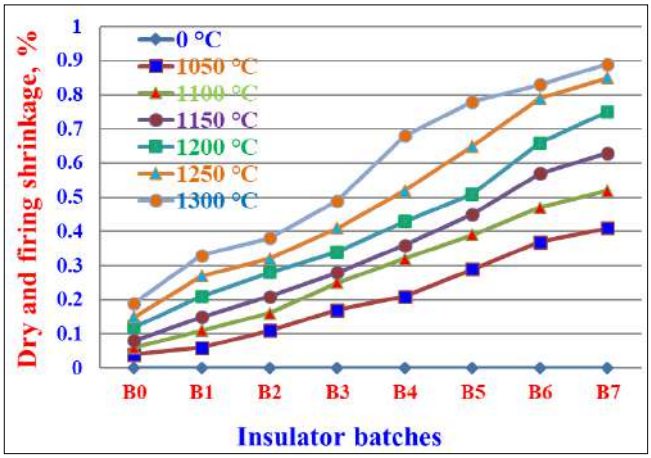

Fig 10: Dry and firing shrinkage of the various dry and fired ceramin insulator batches at different firing temperatures.

4. Conclusions

1. This research studied the exploitation of priceless waste material (SCBA) instead of the expensive feldspar in the preparation of ceramin insulator products.
2. The oxide composition of SCBA is more or less very similar to that of feldspar3- Water absorption and apparent porosity were decreased with both SCBA content and firing temperature.
3. Bulk density was improved and enhanced wotheither SCBA and firing temperature.
4. The same trend in bulk density was displayed with mechanical properties.
5. The dry shrinkage was unchanged, while the firing shrinkage was slightly increased with both SCBA content anf firing temperature.
6. The optimum ceramic insulator batch was that containing 35% SCBA fired at 1300 ºC decause it recoprded the highest results.
7. The higher amount of fluxing oxides (7.83%) in SCBA cpmpared that of F (7.23%) is the main cause that make SCBA was suitable to be replaced F in the production of ceramic insulator products.

5. Declaration of Competing Interest

The author declares that he does not have any commercial or associative interest that represents a conflict of interest in connection with the work submitted.

6. Acknowledgments

The author gratefully acknowledges the financial support of the National Research Centre.

7. Fud: This research article is self-sponsored.

8. References

1. Olupot PW, Jonsson S, Byaruhanga JK. Development and characterisation of triaxial electrical porcelains from Ugandan ceramic minerals, Ceramics International. 2010;36(4):1455-1461. DOI: https://doi.org/10.1016/j.ceramint.2010.02.006.
2. Mehta NS, Sahu PK, Tripathi P, Pyare R, Majhi MR. Influence of alumina and silica addition on the physico-mechanical and dielectric behavior of ceramic porcelain insulator at high sintering temperature, Boletin de la Sociedad Espanola de Ceramica y Vidrio. 2018;57(4):151-159. DOI:

https://doi.org/10.1016/j.bsecv.2017.11.002.
3. Piva RH, Vilarinho P, Morelli MR, Fiori MA, Montedo ORK. Influence of Fe_2O_3 content on the dielectric behavior of aluminous porcelain insulators, Ceramics International. 2013;39(7):7323-7330. DOI: https://doi.org/10.1016/j.ceramint.2013.02.071.
4. Moyo MG, Park E. Ceramic Raw Materials in Tanzania – Structure and Properties for Electrical Insulation Application, International Journal of Engineering Research & Technology (IJERT). 2014;3(10):1015–1020.
5. Demchuk V, Shchekina G, Kostyukov N, Lukichev A, Kalinichenko B. Fabrication of electroporcelain on the basis of raw materials from the Amur region, Glass and Ceramics - Glass Ceram-Engl TR. 2009 Jan;66:63-65. Doi: https://doi.org/10.1007/s10717- 009-9125-7.
6. Islam RA, Chan YC, Islam MF. Structure-property relationship in high-tension ceramic insulator fired at high temperature, Materials Science and Engineering B: Solid-State Materials for Advanced Technology. 2004;106(2):132-140. DOI: https://doi.org/10.1016/j.mseb.2003.09.005.
7. Darweesh HHM. Recycling of glass waste in ceramics — part I: physical, mechanical and thermal properties, SN Applied Sciences. 2019;1(10):1-11. DOI: https://doi.org/10.1007/s42452-019-1304-8.
8. Nwachukwu VC, 483 Lawal S. Investigating the Production Quality of Electrical Porcelain Insulators from Local Materials, IOP Conference Series: Materials Science and Engineering. 2018;413:1-9. DOI: https://doi.org/10.1088/1757-899X/413/1/012076.
9. Belhouchet K, Bayadi A, Belhouchet H, Romero M. Improvement of mechanical and dielectric properties of porcelain insulators using economic raw materials, Boletin de la Sociedad Espanola de Ceramica y Vidrio. 2019;58(1):28-37. DOI: https://doi.org/10.1016/j.bsecv.2018.05.004.
10. De Noni A, Hotza D, Soler VC, Vilches ES. Influence of composition on mechanical behaviour of porcelain tile. Part I: Microstructural characterization and developed phases after firing, Materials Science and Engineering A. 2010;527(7-8):1730-1735. DOI: https://doi.org/10.1016/j.msea.2009.10.057.
11. Ghorbel A, Fourati M, Bouaziz J. Microstructural evolution and phase transformation of different sintered Kaolins powder compacts, Materials Chemistry and Physics. 2008;112(3):876-885. DOI: https://doi.org/10.1016/j.matchemphys.2008.06.047.
12. Bragança S, Bergmann C. Traditional and glass powder porcelain: Technical and microstructure analysis, Journal of the European Ceramic Society. 2004;24(8):2383-2388. DOI: https://doi.org/10.1016/j.jeurceramsoc.2003.08.003.
13. Locks M, Arcaro S, Bergmann CP, Ribeiro MJPMJ, Raupp-Pereira F, Montedo ORK. Effect of feldspar substitution by basalt on pyroplastic behaviour of porcelain tile composition, Materials. 2021;14(14). DOI: https://doi.org/10.3390/ma14143990.
14. Figueirêdo J, Silva J, Neves G, Ferreira H, Santana L. Influence of Processing Variables on Clay-Based Ceramic Formulations, Materials Research. 2019;22:1-9. Doi: http://dx.doi.org/10.1590/1980-5373-MR-2018-0548.
15. Lee WE, Iqbal Y. Influence of mixing on mullite formation in porcelain. 2001;21(14):2583-2586.
16. Andreev DV, Zakharov AI. Ceramic item deformation during firing: effect of composition and microstructure (review), Refractories and Industrial Ceramics. 2009;50(4):298-303. DOI: https://doi.org/10.1007/s11148-009-9191-y.
17. Bragança SR, Bergmann CP, Hübner H. Effect of quartz particle size on the strength of triaxial porcelain, Journal of the European Ceramic Society. 2006;26(16):3761-3768. DOI: http://dx.doi.org/10.1590/1980-5373-MR-2018-0548 Influence.
18. Buchanan RC. Ceramic materials for electronics. New York: Marcel Dekker; c2004.
19. Mukhopadhyay TK, Ghosh S, Ghatak S, Maiti HS. Effect of pyrophyllite on vitrification and on physical properties of triaxial porcelain, Ceramics International. 2006;32(8):871-876. DOI: https://doi.org/10.1016/j.ceramint.2005.07.002.
20. Ochen W. Effect of Quartz Particle Size on Sintering Behavior and Flexural Strength of Porcelain Tiles Made from Raw Materials in Uganda, Advances in Materials. 2019;8(1):33. DOI: https://doi.org/10.11648/j.am.20190801.15.
21. Gaied ME, Gallala W, Essefi E, Montacer M. Microstructural and Mechanical Properties in Traditional Ceramics as a Function of Quartzofeldspathic Sand Incorporation, Transactions of the Indian Ceramic Society. 2011 Oct;70(4):207-214. DOI:10.1080/0371750X.2011.10600170.
22. Ngayakamo B, Park SE. Evaluation of Tanzania local ceramic raw materials for high voltage porcelain insulators production, Ceramica. 2018;64:570-576.
23. Merga A, Murthy H, Amare E, Ahmed K, Bekele E. Fabrication of electrical porcelain insulator from ceramic raw materials of Oromia region, Ethiopia, Heliyon; c2019, 5. DOI: https://doi.org/10.1016/j.heliyon.2019.e02327.
24. Njoya D, Tadjuidje FS, Ndzana EJA, Pountouonchi A, Tessier-Doyen N, Lecomte-Nana G. Effect of flux content and heating rate on the microstructure and technological properties of Mayouom (Western-Cameroon) kaolinite clay based ceramics, Journal of Asian Ceramic Societies. 2017;5(4):422-426. DOI: http://dx.doi.org/10.1016/j.jascer.2017.09.004.
25. Dana K, Das SK. Partial substitution of feldspar by B.F. slag in triaxial porcelain: Phase and microstructural evolution, Journal of the European Ceramic Society. 2004;24(15-16):3833-3839. DOI: https://doi.org/10.1016/j.jeurceramsoc.2004.02.004.
26. Matteucci F, Dondi M, Guarini G. Effect of soda-lime glass on sintering and technological properties of porcelain stoneware tiles, Ceramics International. 2002;28(8):873-880. DOI: https://doi.org/10.1016/S0272-8842(02)00067-6.
27. Aziz DAA, 543 Aly MH, Salem IA, Abead SA. Effect of Air Blast Furnace Slag and γ- Alumina Content on Dielectric Properties and Physical Properties of Porcelain Insulators, Physics and Materials Chemistry. 2015;3(2):30-36. DOI: https://doi.org/10.12691/pmc-3-2-3.
28. Karamanova E, Avdeev G, Karamanov A. Ceramics from blast furnace slag, kaolin and quartz, Journal of the European Ceramic Society. 2011;31(6):989-998.

DOI: https://doi.org/10.1016/j.jeurceramsoc.2011.01.006.
29. Dana K, Das SK. High strength ceramic floor tile compositions containing Indian metallurgical slags, Journal of Materials Science Letters. 2003;22(5):387-389. DOI: https://doi.org/10.1023/A:1022657429358.
30. Prasad CS, Maiti KN, Venugopal R. Effect of rice husk ash in whiteware compositions, Ceramics International. 2001;27(6):629-635. DOI: https://doi.org/10.1016/S0272- 8842(01)00010-4
31. Prasad CS, Maiti KN, Venugopal R. Effect of silica fume addition on the properties of whiteware compositions, Ceramics International. 2002;28(1):9-15. DOI: https://doi.org/10.1016/S0272-8842(01)00051-7.
32. Dana K, Das SK. Evolution of microstructure in flyash-containing porcelain body on heating at different temperatures, Bulletin of Materials Science. 2004;27(2):183-188. DOI: https://doi.org/10.1007/BF02708503.
33. Darweesh HHM. Ceramic Wall and Floor Tiles Containing Local Waste of Cement Kiln Dust - Part I: Densification Parameters, American Journal of Environmental Engineering and Science. 2015;2(5):35-43. http://www.aascit.org/journal/ajees.
34. Darweesh HHM. Ceramic Wall and Floor Tiles Containing Local Waste of Cement Kiln Dust- Part II: Dry and Firing Shrinkage as well as Mechanical Properties, American Journal of Civil Engineering and Architecture. 2016;4(2):44-49. DOI:10.12691/ajcea-4-2-1.
35. Fairbairn EMR, Americano BB, Cordeiro GC, Paula TP, Toledo Filho RD, Silvoso MM. Cement replacement by sugar cane bagasse ash: CO_2 emissions reduction and potential for carbon credits, Journal of Environmental Management. 2010;91(9):1864-1871. DOI: 10.1016/j.jenvman.2010.04.008.
36. Arif E, Clark MW, Lake N. Sugar cane bagasse ash from a high-efficiency co-generation boiler as filler in concrete, Construction and Building Materials. 2017;151:692-703. DOI: http://dx.doi.org/10.1016/j.conbuildmat.2017.06.136.
37. Xu Q, Ji T, Gao SJ, Yang Z, Wu N. Characteristics and Applications of Sugar Cane Bagasse Ash Waste in Cementitious Materials, Materials (Basel, Switzerland). 2018;12(1):1-19. DOI: https://doi.org/10.3390/ma12010039.
38. Faria K, Holanda J. Incorporation of sugarcane bagasse ash waste as an alternative raw material for red ceramic, Cerâmica. Sep. 2013;59:473-480. DOI: https://doi.org/10.1590/S0366-69132013000300019.
39. Sales A, Lima SA. Use of Brazilian sugarcane bagasse ash in concrete as sand replacement, Waste Management. 2010;30(6):1114-1122. DOI: https://doi.org/10.1016/j.wasman.2010.01.026.
40. Junkes JA, Prates PB, Hotza D, Segadães AM. Combining mineral and clay-based wastes to produce porcelain-like ceramics: An exploratory study, Applied Clay Science. 2012;69:50-57. http://dx.doi.org/10.1016/j.clay.2012.08.009.
41. Souza AE, Teixeira SR, Santos GTA, Costa FB, Longo E. Reuse of sugarcane bagasse ash (SCBA) to produce ceramic materials, Journal of Environmental Management. 2011;92(10):2774-2780. https://doi.org/10.1016/j.jenvman.2011.06.020.
42. Darweesh HHM. A Review Article on the Influence of the Electrostatic Precipitator Cement Kiln Dust Waste on the Environment and Public Health, Composite Materials. 2017;2(1):8-14. http://www.sciencepublishinggroup.com/j/cm.
43. Darweesh HHM, Wahsh MMS, Negim EM. Densification and Thermomechanical Properties of Conventional Ceramic Composites Containing Two Different Industrial Byproducts, American-Eurasian Journal of Scientific Research. 2014;7(3):123-130. DOI: 10.5829/idosi.aejsr.2012.7.3.1104.
44. Darweesh HHM. Recycling of Glass Waste in Ceramics-Part II: Microstructure of Ceramic Products using XRD, DTA and SEM Techniques, Research & Development in Material science, (RDMS). 2020;13(4):1424-1431. DOI: 10.31031/RDMS.2020.13.000817.
45. Darweesh HHM. Glass waste as a flux instead of feldspar in Ceramic tiles- Part III, Journal of Current Engineering and Technology. 2020;2(2):128-134. www.pubtexto.com.
46. Wahsh MMS, Sadek HEH, Abd El-Aleem S, Darweesh HHM. The Effect of Microsilica and Aluminum Metal Powder on the Densification Parameters, Mechanical Properties and Microstructure of Alumina–Mullite Ceramic Composites, Advances in Materials. 2015;4(4):80-84. DOI: 10.11648/j.am.20150404.12.
47. Darweesh HHM. Nanoceramics: Materials, Properties, Methods and Applications-Part II, Nanoscience. 2018;1(1):40-66. www.itspoa.com/journal/nano.
48. Chiang YM, Birnie DP, Kingery WG. Physical Ceramics-Principals for Ceramic Science and Engineering", 3rd edn., John Wiley and Sons, Lehigh Press. Inc., USA; c1997.
49. Ezenwabude E, Madueme T. Evaluation of Mixed Local Materials for Low Voltage Insulators, International Journal of Multidisciplinary sciences and Engineering. 2015;6:28-38.
50. Yaya A, Tiburu EK, Vickers ME, Efavi JK, Onwona-Agyeman B, Knowles KM. Characterisation and identification of local kaolin clay from Ghana: A potential material for electroporcelain insulator fabrication, Applied Clay Science. 2017;150:125-130. doi: https://doi.org/10.1016/j.clay.2017.09.015.
51. Gaied ME, Gallala W, Essefi E, Montacer M. Microstructural and Mechanical Properties in Traditional Ceramics as a Function of Quartzofeldspathic Sand Incorporation, Transactions of the Indian Ceramic Society. 2011;70(4):207-214. DOI: 10.1080/0371750X.2011.10600170.
52. ASTM-C373-72. Standard Test Method for water absorption, bulk density, apparent porosity and specific gravity of white ware products", Reapproved 1980;(Part 17):308-309.
53. ASTM-C373-88. Standard Test Method for Water Absorption, Bulk Density, Apparent Porosity, and Apparent Specific Gravity of Fired Whiteware Products," 1999, Astm C373-88, Vol. 88, no. Reapproved, 1-2.
54. ASTM-C78-02. Standard Test Method for flexural strength of concrete using simple Beam with Three-Points Loading system; c2002. p. 1-3.
55. ASTM-D790-17. Standard Test Methods for Flexural Properties of Unreinforced and Reinforced Plastics and

Electrical Insulating Materials. 2002;1:1-12.
56. ASTM-C170-90. Standard test method for cold crushing strength of dimensional stones; c1990. p. 828-830.
57. Jara AD, Woldetinsae G, Betemariam A, Kim JY. Mineralogical and petrographic analysis on the flake graphite ore from Saba Boru area in Ethiopia," International Journal of Mining Science and Technology. 2020;30(5):715-721. DOI: https://doi.org/10.1016/j.ijmst.2020.05.025.
58. Mahmoudi S, Bennour A, Srasra E, Zargouni F. Characterization, firing behavior and ceramic application of clays from the Gabes region in South Tunisia, Applied Clay Science; c2016, 135. DOI: http://dx.doi.org/10.1016/j.clay.2016.09.023.
59. Carty W, Senapati U. Porcelain-Raw Materials, Processing, Phase Evolution, and Mechanical Behavior. Journal of the American Ceramic Society. 1998;81(1):3-20. DOI: https://doi.org/10.1111/j.1151-2916.1998.tb02290.x.
60. Meng Y, Gong G, Wu ZP, Yin ZJ, Xie YM, Liu SR. Fabrication and microstructure investigation of ultra-high-strength porcelain insulator, Journal of the European Ceramic Society. 2012;32(12):3043-3049. DOI: http://dx.doi.org/10.1016/j.jeurceramsoc.2012.04.015.
61. Tsozué D, Nzeugang AN, Mache JR, Loweh S, Fagel N. Mineralogical, physico chemical and technological characterization of clays from Maroua (Far-North, Cameroon) for use in ceramic bricks production, Journal of Building Engineering; 2017 Mar 11. p. 17-24. DOI: http://dx.doi.org/10.1016/j.jobe.2017.03.008.
62. Kimambo V. Suitability of Tanzanian Kaolin, Quartz and Feldspar as Raw Materials for the Production of Porcelain Tiles, International Journal of Science, Technology and Society. 2014;2(6):201-208. DOI: https://doi.org/10.11648/j.ijsts.20140206.17.
63. Anbalagan G, Prabakaran AR, Gunasekaran S. Spectroscopic characterization of indian standard sand, Journal of Applied Spectroscopy. 2010 Mar;77:86-94. DOI: https://doi.org/10.1007/s10812-010-9297-5.
64. Ece OI, Nakagawa ZE. Bending strength of porcelains, Ceramics International. 2002;28(2):131-140. DOI: https://doi.org/10.1016/S0272-8842(01)00068-2.
65. Agredo J, Mejia R, Giraldo C, González Salcedo L. Characterization of sugar cane bagasse ash as supplementary material for Portland cement, Ingenieria e Investigacion. 2014;34(1):5-10. DOI: https://doi.org/10.15446/ing.investig.v34n1.42787.
66. Pontikes Y, Esposito L, Tucci A, Angelopoulos GN. Thermal behaviour of clays for traditional ceramics with soda-limesilica waste glass mixture. J Eur Ceram Soc. 2007;27(2-3):1657-1663.
67. Luz AP, Ribeiro S. Use of glass waste as a raw material in porcelain stoneware tile mixtures. Ceram Int. 2007;33(5):761-765.
68. Elwan M, Abdel-Aziz D, El-Didimony H. Effect of by pass cement dust on the properties of clay bricks. Ceramic Silikaty. 1999;43(3):117-121.
69. Kr Das S, Dana K, Singh N, Sarkar R. Shrinkage and strength behaviour of quartzitic and kaolinitic clays in wall tile compositions. Applied Clay Science. 2005;29(2):137-143.
70. Souza AJ, Pinheiro BCA, Holanda JNF. Recycling of gneiss rock waste in the manufacture of vitrified floor tiles, Environm. Management J. 2010;91(3):685-689.
71. Moroz BI, Gumenyuk AE, Mel'nikov VM, Trubachov VI. Bodies for the manufactureof ceramic tiles, Stroit.Mater. Konstr. USSR. 1990;2:17.